

Boundary slip as a result of a prewetting transition

Denis Andrienko,¹ Burkhard Dünweg,¹ and Olga I. Vinogradova^{1,2}

¹Max-Planck-Institut für Polymerforschung, Ackermannweg 10, D-55128 Mainz, Germany

²Laboratory of Physical Chemistry of Modified Surfaces, Institute of Physical Chemistry, Russian Academy of Sciences, 31 Leninsky Prospect, 119991 Moscow, Russia

(Dated: February 21, 2019)

Some fluids exhibit anomalously low friction when flowing against a certain solid wall. To recover the viscosity of a bulk fluid, slip at the wall is usually postulated. On a macroscopic level, a large slip length can be explained as a formation of a film of gas or phase-separated ‘lubricant’ with lower viscosity between the fluid and the solid wall. Here we justify such an assumption in terms of a prewetting transition. In our model the thin-thick film transition together with the viscosity contrast gives rise to large boundary slip. The calculated value of the slip length has a jump at the prewetting transition temperature which depends on the strength of the fluid-surface interaction (contact angle). Furthermore, the temperature dependence of the slip length is non-monotonous.

PACS numbers: 47.10.+g, 68.08.-p, 81.40.Pq

I. INTRODUCTION

It is accepted in hydrodynamics that the velocity of the liquid immediately adjacent to a solid is equal to that of the solid [1]. Such an absence of a jump in the velocity of a simple liquid at a surface seems to be a confirmed fact in *macroscopic* experiments. However, it is difficult to obtain the same conclusion using *microscopic* models. It has been noticed that, even in case of simple liquids, the no-slip boundary condition is not justified on a microscopic level.

Therefore, the conventional condition of continuity of the velocity, or the *no-slip* boundary condition, is not an exact law but a statement of what may be expected to happen in normal circumstances. While the normal component of the liquid velocity must vanish at an impermeable wall for kinematic reasons, the requirement of no-slip can be relaxed. In other words, instead of imposing a zero tangential component of the liquid velocity at the solid, it is possible to allow for an amount of slippage, described by a slip length b . The slip length for a simple shear flow is the distance behind the interface at which the liquid velocity extrapolates to zero

$$v_s = b(\partial_z v)_{\text{wall}}, \quad (1)$$

where v_s is the tangential velocity at the wall, and the z axis is perpendicular to the surface. The definition of b is explained in Fig. 1. It is clear that the boundary slip is important only when the length-scale over which the liquid velocity changes approaches the slip length. Therefore, it is not surprising that the slippage effect has not been detected in macroscopic experiments. In microfluidic devices, however, where the liquid is highly confined, the boundary slip is important [2].

Indeed, water flow in capillaries of small diameter with smooth hydrophobic walls has been investigated and slip at the wall had to be postulated to recover the viscosity of water [3, 4]. These results were confirmed by directly probing the fluid velocity at a solid surface using total

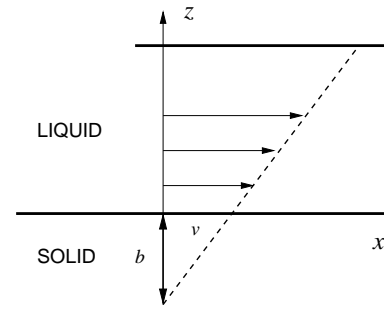


FIG. 1: Definition of the slip length b for a simple shear flow.

internal reflection-fluorescence recovery [5, 6] as well as double focus fluorescence cross-correlation [7]. Several indirect methods were also used: the quartz-crystal microbalance (QCM) [8], the surface force apparatus (SFA) [9, 10, 11, 12], and the atomic force microscope (AFM) [13]. The magnitude of the slip length b was sometimes greater than 100 nm for partially wetted walls [5, 10]. In some cases the shear rate did not affect the amount of slip in the observed range [5]; in others a strong dependence on the velocity was found [9, 10]. It was also shown that both surface roughness and strength of the fluid-surface interactions affect the wall slip [3, 11].

The no-slip condition can also be violated in more complex systems. Boundary slip has been suggested for polymer melts [14, 15, 16] and liquid crystals [17] (for the rotational motion of molecules).

The origin of such large slippages remains unclear despite considerable theoretical effort. On the theoretical side, molecular dynamics simulations have shown that the molecules can slip directly over the solid due to the fact that the strength of attraction between the liquid molecules is greater than the competing solid-liquid interaction [18, 19, 20, 21, 22, 23]. In general, wall slip was found on non-wetting surfaces, i.e. when the contact angle is large. However, the simulation results were

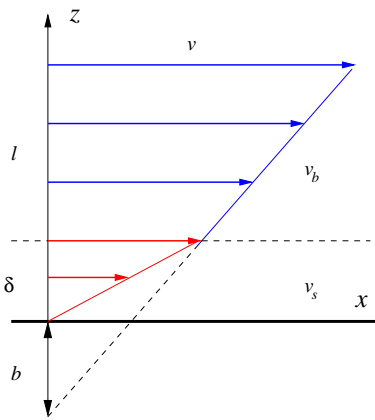


FIG. 2: Slip length b for a binary mixture.

not entirely consistent with the experimental data, by predicting a much lower slip length [24, 25] and at a larger contact angle [23]. It has also been demonstrated that the surface roughness may both reduce [26] and increase [27, 28] friction of the fluid past the boundaries.

Other ideas invoke the formation of a new phase at the wall. The possible source of the surface layer could be a gas (lubricant) dissolved in the liquid at a metastable concentration. Because of the pressure drop in the slab this new phase can form bubbles nucleating at the liquid/solid interface [29, 30, 31]. Experimental evidence for the formation of a wetting layer under flow has been observed by Tanaka [32, 33]. The boundary layer can have a lower viscosity than the bulk value [34]. Tuning the size and the properties of this layer one can obtain large values of the slip length (see Fig. 2). Indeed, in a sharp interface limit, when the width of the interface is much smaller than the width of the gap and thickness of the boundary layer, we can neglect the structure of the interface and use the condition of zero divergence of the stress tensor. Then the problem is reduced to the flow of incompressible fluid in a slab with corresponding boundary conditions at the wall and the phase separation boundary (see Fig. 2)

$$\partial_z (\eta(z) \partial_z v) = 0, \quad (2)$$

$$v_b(\delta) = v_s(\delta); \quad v_b(l + \delta) = v \quad (3)$$

$$v_s(0) = 0; \quad \eta_s v'_s(\delta) = \eta_b v'_b(\delta) \quad (4)$$

where $\eta(z)$ is the viscosity, which in this case is a step function: $\eta = \eta_b$ in the bulk and $\eta = \eta_s$ in the boundary layer, $v(z)$ is the velocity profile, $v' = \partial v / \partial z$.

The solution in the bulk

$$v_b = \kappa v \left(\frac{\eta_b}{\eta_s} - 1 + \frac{z}{\delta} \right), \quad (5)$$

where $\kappa = (\eta_b / \eta_s + l / \delta)^{-1}$, allows for a slip length

$$b = \delta \left(\frac{\eta_b}{\eta_s} - 1 \right), \quad (6)$$

where δ is the thickness of the boundary layer.

According to Eq. (6) the boundary slip can be observed if the viscosity depends on the composition ($\eta_b \neq \eta_s$) and the less viscous fraction of the liquid wets the walls better than the more viscous one ($\eta_b > \eta_s$). It is also clear that there are two ways to obtain a large slip length. First, by having a macroscopically thick boundary layer, since the slip length has the same order of magnitude as the thickness of this layer. Second, by providing large values of the viscosity contrast η_b / η_s , e.g. for a gas layer [60].

A more realistic description should allow for a prewetting transition [35, 36] for the liquid/gas or liquid/lubricant mixture and take into account the structure and the finite width of the interface region. The aim of this paper is to include these effects and relate the slip length to the wettability of the walls, composition of the mixture, and thermodynamic parameters of the system. We show that the prewetting transition can give rise to a large boundary slip of the fluid by generating a thick film of a phase-separated ‘lubricant’ at the wall which has a lower than the bulk fluid viscosity. Indeed, if we choose typical values, thickness of the wetting layer (thick film) $\delta \approx 10\text{nm}$, viscosity contrast $\eta_b : \eta_s = 3 : 1$, we find $b \approx 20\text{nm}$, i.e. the prewetting film can indeed give a large slip length. This value can be further increased since the thickness of the wetting layer increases with the temperature, $\delta \propto -\ln(T_t - T)$ for short-range forces [36].

The paper is organized as follows. In Sec. II we outline the phase-field approach that allows us to calculate the phase diagram, order parameter profiles, and slip length. Section III gives a summary of the results. Finally, in Sec. IV, we present some brief conclusions.

II. PHASE-FIELD APPROACH

Phase separation phenomena in binary and polymer mixtures have been intensively studied by theory, experiment, and simulation. While the most detailed information is available for the static bulk behavior, much more interesting phenomena occur when studying the dynamics [37, 38, 39, 40] or the behavior near surfaces or in confined geometries [35, 41, 42, 43]. The theoretical understanding of phenomena which combine both aspects (i. e. dynamics near surfaces) is still at its infancy [44], while there are many experiments [33, 34, 45].

To describe the bulk phase as well as the interface structure, ‘phase-field’ models [35] are often used. In this approach the order parameter ϕ (for a binary mixture it is the density difference of the two phases) is introduced. This order parameter varies slowly in the bulk regions and rapidly on length scales of the interfacial width. The free energy functional $\mathcal{F}(\phi)$ determines the *bulk* phase behavior. Since the material is confined in a container in any experiment, phase separation is always affected by surface effects [46, 47, 48, 49, 50]. To include them, appropriate surface terms responsible for the interaction of

the liquid with the container walls shall be added to the free energy [35, 36, 42, 51, 52, 53].

In the phase-field approach the grand potential of a binary mixture can be written as [36]

$$\Omega\{\phi\} = \int dV \left[\frac{k}{2} (\nabla\phi)^2 + f(\phi) - \Delta\mu\phi \right] + \Psi_s, \quad (7)$$

where $f(\phi)$ is the Helmholtz free energy density of the mixture, $\phi = \phi_1 - \phi_2$ is the order parameter, $\phi_i = n_i/(n_1 + n_2)$ are the mole fractions of particles of type 1 and 2, $\Delta\mu = \mu_1 - \mu_2$ is the difference of chemical potentials which allows one to tune the bulk value of the order parameter ϕ , and Ψ_s is the surface energy.

The explicit form of the Helmholtz free energy $f(\phi)$ varies depending on the mixture. However, the simple observation that the two phases must coexist implies that there are two minima in the free energy at the respective values of the order parameter of the phases α and β . For a *regular mixture* the free energy $f(\phi)$ is given by [54, 55]

$$f(\phi) = \frac{\chi}{4}(1 - \phi^2) + k_B T \left[\frac{1 + \phi}{2} \ln \frac{1 + \phi}{2} + \frac{1 - \phi}{2} \ln \frac{1 - \phi}{2} \right], \quad (8)$$

where the first term on the right-hand side corresponds to the excess energy of mixing.

To describe the interaction with the walls we used the quadratic approximation for the surface energy [36, 56]

$$\Psi_s = \int \left[-h\phi_s - \frac{1}{2}\gamma\phi_s^2 \right] dS, \quad (9)$$

where ϕ_s is the surface value of the order parameter and the parameters h and γ are referred to as the short-range surface field and the surface enhancement, respectively. The short-range surface field, h , is a measure of the attractiveness (or repulsiveness, if negative) of the surface by the component 1, due to the choice of the order parameter in the form $\phi = \phi_1 - \phi_2$. In real systems it can be of either sign and of any magnitude. The surface coupling enhancement, γ , represents the effect that a molecule close to the substrate has fewer neighbors than a molecule in the bulk; γ is estimated to be small and negative. We have implicitly assumed that all surface effects are of short range, thus f_s depends on the local concentration at the walls only. Because of long range van der Waals forces this is not fully realistic. However, for large enough wall separations the differences to the short range case are rather minor.

In thermal equilibrium the grand potential (7) must be minimal. Variation of this functional yields an Euler-Lagrange equation together with two boundary conditions. In the geometry with two symmetric walls it is convenient to choose the origin of the coordinates at the center of the film. Then the Euler-Lagrange equations

and boundary conditions read

$$\frac{\partial^2\phi}{\partial z^2} + \frac{1}{2}\phi - \frac{1}{2}T \ln \frac{1 + \phi}{1 - \phi} + \Delta\mu = 0, \quad (10)$$

$$\pm \frac{\partial\phi}{\partial z} + h + \gamma\phi \Big|_{z=-L/2, L/2} = 0, \quad (11)$$

where we introduced dimensionless units by putting $k_B = 1$, $k = 1$, $\chi = 1$. In these units the temperature is measured in units χ/k_B , chemical potential in χ , coordinate in $\sqrt{\chi/k}$, etc.

To obtain the order parameter profiles the boundary-value problem of Eqs. (10,11) was solved using the relaxation method [57]. In general the boundary problem can have up to three different solutions: one stable, one metastable, and one unstable. The relaxation method yields only two of them: a *metastable* and a *stable* solution. The unstable solution with the highest free energy has negative response function $(\partial\phi/\partial\mu)_T$ and is eliminated by the relaxation method automatically.

To select stable solutions, we calculated the grand potential of the mixture, Ω , for both stable and metastable solutions and picked up the solution with the lowest grand potential. This allows the accurate determination of the phase diagram.

To calculate the velocity profiles, we assumed that the viscosity of the system is a linear combination of that of the individual components

$$\eta(z) = \eta_s \frac{1 + \phi(z)}{2} + \eta_b \frac{1 - \phi(z)}{2}, \quad (12)$$

where the viscosity contrast between the two components has been chosen as $\eta_s : \eta_b = 1 : 3$. The stationary velocity profile is the solution of Eq. (2)

$$v = v_0 c^{-1} \int_{-L/2}^z \frac{dz}{\eta(z)}, \quad (13)$$

where $c = \int_{-L/2}^{L/2} \frac{dz}{\eta(z)}$. The value of the slip length was calculated from Eq. (1) where $v(z)$ was obtained by fitting the *bulk* region of the velocity profile (13) with a linear regression.

Note that our approach splits the problem of shear flow of a binary mixture into two independent tasks. First we calculate the equilibrium order parameter profiles. Then the stationary velocity profile is calculated from the order parameter profile. We justify this approach in Appendix A.

III. RESULTS AND DISCUSSION

A. Order parameter profiles and prewetting phase diagram

Typical order parameter profiles at the same value of the chemical potential difference $\Delta\mu = -0.002$ and a

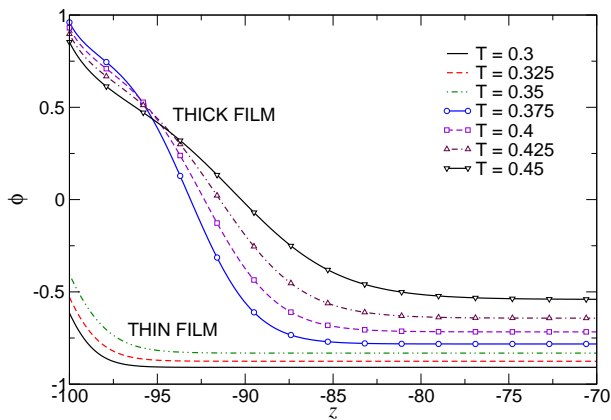


FIG. 3: Typical order parameter profiles. Only the part next to the wall is shown. Thickness of the slab $L = 200$, $\Delta\mu = -0.002$, $\gamma = -0.01$, $h = 0.2$. For this chemical potential difference the thin-thick film transition occurs at $T \approx 0.35$.

set of temperatures are shown in Fig. 3. Only the profiles corresponding to the stable thermodynamic state are shown. The profiles have a well-developed flat region in the center of the film, which indicates that there should not be finite size effects for the chosen thickness of the slab ($L = 200$). This flat region is important for using the definition of the slip length in the form (1), which requires a well-defined region of the *bulk* phase.

Following the change in the profiles with the temperature, one clearly sees the thin-thick film transition close to $T = 0.35$. From these profiles, taking into account the remarks made in the introduction and Eq. (6), we can already anticipate small slip lengths for thin films and large slip lengths for thick films (above the prewetting transition temperature). Since the thin-thick film transition is a first-order transition, one can also expect a jump in the slip length at the prewetting transition temperature.

To calculate the thin-thick film transition temperature, we followed the metastable solution up to its stability limit (spinodal) calculating the grand potential for both stable and metastable solutions. The transition line was determined from the intersection of grand potentials of stable and metastable solutions (thick and thin films). Both spinodals as well as the transition line are shown in a prewetting transition phase diagram, Fig. 4. The solid curve is the prewetting curve ending at the prewetting critical point and the dashed curves are spinodals or metastability limits of the metastable states.

B. Slip length

The temperature dependence of the slip length for several values of the chemical potential difference (or average volume fraction) is presented in Fig. 5. As we anticipated, $b(T)$ has a jump at the prewetting transition temperature, when the thick film is formed (path I in Fig. 4).

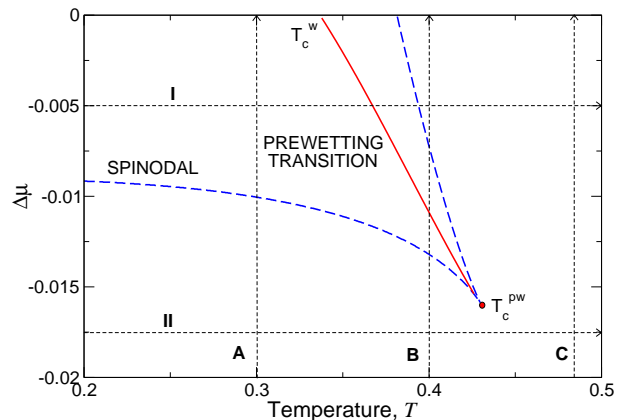


FIG. 4: Prewetting phase diagram calculated for $h = 0.2$, $\gamma = -0.01$, $L = 200$. The solid line is the prewetting transition line ending at the prewetting critical point. Metastability limits of thick and thin films (spinodals) are shown with dashed lines. A, B, C, I, and II are thermodynamic paths used in the text.

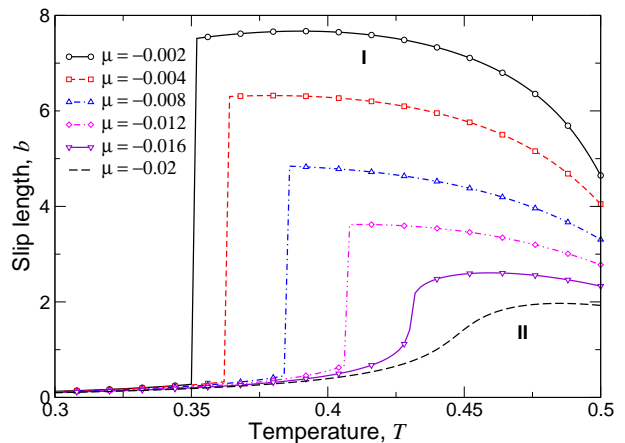


FIG. 5: Slip length vs. temperature calculated for several values of the chemical potential. $h = 0.2$, $\gamma = -0.01$, $L = 200$.

Before the jump the slip length is small and practically does not depend on temperature. After the transition the slip length decreases with the temperature increasing, even though the prewetting film gets thicker. This is because the bulk volume fraction (order parameter ϕ) increases, giving rise to a decrease in the bulk viscosity (or, equivalently, viscosity contrast) (see Fig. 3). If we are above the prewetting critical point (path II in Fig. 4) there is no jump-like transition, but rather a smooth increase of the slip length with the temperature.

The dependence of the slip length on the chemical potential difference is shown in Fig. 6. If the temperature is below T_c^w then the thin film is always stable and the slip length is small (path A in Fig. 4). Once we intersect the prewetting transition line, the thick film forms with the increase of the average fraction of the more wettable

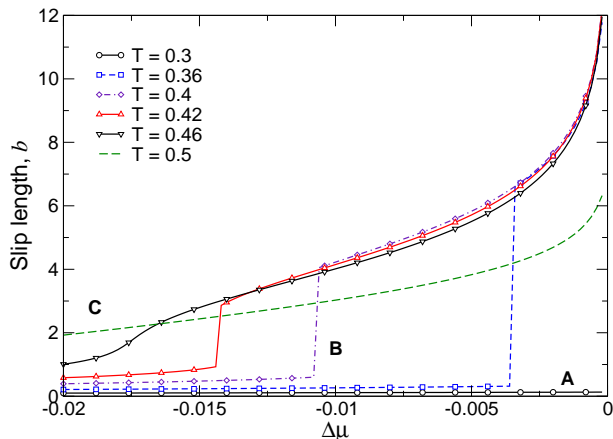


FIG. 6: Slip length vs. chemical potential difference. $h = 0.2$, $\gamma = -0.01$, $L = 200$.

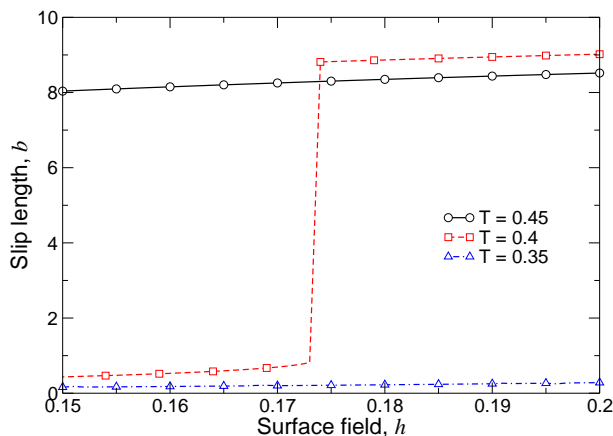


FIG. 7: Slip length vs. short-range surface field. $\Delta\mu = -0.001$.

phase (values of the chemical potential close to zero) and the slip length jumps abruptly to higher values (path B in Fig. 4). Above the prewetting critical point T_c^{pw} the slip length increases monotonically with the increase of the chemical potential difference (see path C in Fig. 4).

Finally, the dependence of the slip length on the surface field h is shown in Fig. 7. It is clear that there is a threshold value of the surface field (contact angle) when the thick film is formed. At this value of the surface field the slip length increases abruptly. Below the threshold the slip length is small and practically does not depend on the surface field.

IV. CONCLUSIONS

To summarize, when the prewetting transition occurs in a flow experiment, it may indeed generate a strong slippage. Prewetting provides a mechanism of generating a macroscopically thick film at the wall. If this film has a

lower viscosity than the bulk value, a strong slippage can be observed above the prewetting transition temperature. The value of the slip length has a jump-like dependence on temperature, concentration of the phase-separated liquid, and surface field (contact angle).

The mean-field model of wetting is rather general and can be applied to liquid-gas systems, binary mixtures, as well as incompressible polymer mixtures in the long wavelength approximation [56]. This implies that the large boundary slip due to prewetting can be observed in all these systems.

Another goal of this paper is to stimulate accurate quantitative measurements of the slip length combined with measurements of the fluid wetting properties. This will allow to study underlying microscopic mechanisms of slippage and choose an adequate model for every experimental situation.

APPENDIX A: VELOCITY PROFILE

The kinetics of phase separating fluids can be described by Model H as follows [58, 59]

$$\begin{aligned} \partial_t \varphi + \nabla \cdot (\varphi \mathbf{v}) &= \Gamma \nabla^2 \mu, \\ \rho \partial_t \mathbf{v} &= \left\{ \nabla \left[\eta \left(\nabla \mathbf{v} + \nabla \mathbf{v}^T \right) \right] - \varphi \nabla \mu \right\}_{\perp}, \end{aligned} \quad (\text{A1})$$

where $\varphi = \rho(\phi_1 - \phi_2)$ is the local concentration difference between the two components, \mathbf{v} is the local velocity, $\mu = \delta F\{\varphi\}/\delta\varphi$. The first equation is the time-dependent Ginzburg-Landau equation, which governs the evolution of the order parameter. The second equation is the Navier-Stokes equation describing the time evolution of the local velocity. $[\dots]_{\perp}$ denotes the transverse operator, ρ is the density, η is the viscosity. $F\{\varphi\}$ is the free energy functional of the system

$$F\{\varphi\} = \int dV \left[\frac{k}{2} (\nabla \varphi)^2 + f(\varphi) \right]. \quad (\text{A2})$$

In a shear geometry $\mathbf{v} = (v(z), 0, 0)$, $\varphi = \varphi(z)$. Then, in the stationary case, equations (A1) read

$$\partial^2 \mu / \partial z^2 = 0, \quad (\text{A3})$$

$$\partial_z (\eta (\partial_z v)) - \varphi \partial_z \mu = 0. \quad (\text{A4})$$

The first equation can be rewritten in the form $\mu = \Delta\mu \equiv \text{const}$ which is the condition for the minimum of the grand potential $\Omega\{\phi\}$. Then the second equation reduces to Eq. (2).

ACKNOWLEDGMENTS

We are grateful to R. Evans, F. Feuillebois, K. Kremer, M. Müller, and J. Vollmer for useful discussions. DA acknowledges the support of the Alexander von Humboldt Foundation.

-
- [1] G. K. Batchelor, *An Introduction to Fluid Dynamics* (Cambridge University Press, Cambridge, 2000).
- [2] O. I. Vinogradova, *Int. J. Miner. Process.* **56**, 31 (1999).
- [3] N. V. Churaev, V. D. Sobolev, and A. N. Somov, *J. Colloid Interface Sci.* **97**, 574 (1984).
- [4] K. Watanabe, Y. Udagawa, and H. Udagawa, *J. Fluid Mech.* **381**, 225 (1999).
- [5] R. Pit, H. Hervet, and L. Leger, *Phys. Rev. Lett.* **85**, 980 (2000).
- [6] D. C. Tretheway and C. D. Meinhart, *Phys. Fluids* **14**, L9 (2002).
- [7] D. Lumma, A. Best, A. Gansen, F. Feuillebois, J. O. Rädler, and O. I. Vinogradova, *Phys. Rev. E* **67**, 056313 (2003).
- [8] J. Krim, *Sci. Am.* **275**, 48 (1996).
- [9] R. G. Horn, O. I. Vinogradova, M. E. Mackay, and N. Phan-Thien, *J. Chem. Phys.* **112**, 6424 (2000).
- [10] Y. X. Zhu and S. Granick, *Phys. Rev. Lett.* **87**, 096105 (2001).
- [11] Y. X. Zhu and S. Granick, *Phys. Rev. Lett.* **88**, 106102 (2002).
- [12] J. Baudry, E. Charlaix, A. Tonck, and D. Mazuyer, *Langmuir* **17**, 5232 (2001).
- [13] V. S. J. Craig, C. Neto, and D. R. M. Williams, *Phys. Rev. Lett.* **87**, 054504 (2001).
- [14] F. Brochard and P. G. de Gennes, *Langmuir* **8**, 3033 (1992).
- [15] A. Ajdari, F. Brochard-Wyart, P. G. de Gennes, L. Leibler, J. L. Viovy, and M. Rubinstein, *Physica A* **204**, 17 (1994).
- [16] F. Brochard-Wyart, C. Gay, and P. G. deGennes, *Macromolecules* **29**, 377 (1996).
- [17] O. Francescangeli, F. Simoni, S. Slussarenko, D. Andrienko, V. Reshetnyak, and Y. Reznikov, *Phys. Rev. Lett.* **82**, 1855 (1999).
- [18] M. Sun and C. Ebner, *Phys. Rev. A* **46**, 4813 (1992).
- [19] M. Sun and C. Ebner, *Phys. Rev. Lett.* **69**, 3491 (1992).
- [20] L. Bocquet and J.-L. Barrat, *Phys. Rev. Lett.* **70**, 2726 (1993).
- [21] P. A. Thompson and S. M. Troian, *Nature* **389**, 360 (1997).
- [22] J. L. Barrat and L. Bocquet, *Faraday Discuss.* **112**, 119 (1999).
- [23] J. L. Barrat and L. Bocquet, *Phys. Rev. Lett.* **82**, 4671 (1999).
- [24] M. Cieplak, J. Koplik, and J. R. Banavar, *Phys. Rev. Lett.* **86**, 803 (2001).
- [25] V. P. Sokhan, D. Nicholson, and N. Quirke, *J. Chem. Phys.* **115**, 3878 (2001).
- [26] C. Cottin-Bizonne, J. L. Barrat, L. Bocquet, and E. Charlaix, *Nat. Mater.* **2**, 237 (2003).
- [27] L. M. Hocking, *J. Fluid Mech.* **76**, 801 (1976).
- [28] I. V. Ponomarev and A. E. Meyerovich, *Phys. Rev. E* **67**, 026302 (2003).
- [29] E. Ruckenstein and P. Rajora, *J. Colloid Interface Sci.* **96**(2), 488 (1983).
- [30] P. G. de Gennes, *Langmuir* **18**, 3413 (2002).
- [31] O. I. Vinogradova, N. F. Bunkin, N. V. Churaev, O. A. Kiseleva, A. V. Lobeyev, and B. W. Ninham, *J. Colloid Interface Sci.* **173**, 443 (1995).
- [32] H. Tanaka, *J. Phys.-Condens. Matter* **13**, 4637 (2001).
- [33] H. Tanaka, *Phys. Rev. Lett.* **70**, 53 (1993).
- [34] O. I. Vinogradova, *Langmuir* **11**, 2213 (1995).
- [35] K. Binder, in *Phase Transitions and Critical Phenomena*, edited by C. Domb and J. Lebowitz (Academic Press, 1983), vol. 8, pp. 2–144.
- [36] D. Bonn and D. Ross, *Rep. Prog. Phys.* **64**, 1085 (2001).
- [37] J. D. Gunton, M. S. Miguel, and P. S. Sahni, in *Phase Transitions and Critical Phenomena*, edited by C. Domb and J. Lebowitz (Academic Press, 1983), vol. 8, p. 269.
- [38] A. J. Bray, *Adv. Phys.* **43**, 357 (1994).
- [39] A. J. Wagner and J. M. Yeomans, *Phys. Rev. Lett.* **80**, 1429 (1998).
- [40] V. M. Kendon, J. C. Desplat, P. Bladon, and M. E. Cates, *Phys. Rev. Lett.* **83**, 576 (1999).
- [41] K. Binder, D. P. Landau, and M. Müller, *J. Stat. Phys.* **110**, 1411 (2003).
- [42] S. Dietrich, in *Phase Transitions and Critical Phenomena*, edited by C. Domb and J. Lebowitz (Academic Press, 1988), vol. 12, p. 1.
- [43] B. Dünweg, D. P. Landau, and A. I. Milchev, eds., *Computer simulations of surfaces and interfaces* (Kluwer, Dordrecht, 2003, to appear).
- [44] S. Puri and K. Binder, *Phys. Rev. E* **49**, 5359 (1994).
- [45] H. Tanaka, *Phys. Rev. Lett.* **70**, 3524 (1993).
- [46] R. Evans, U. M. B. Marconi, and P. Tarazona, *J. Chem. Phys.* **84**, 2376 (1986).
- [47] R. Evans and U. M. B. Marconi, *J. Chem. Phys.* **86**, 7138 (1987).
- [48] L. D. Gelb and K. E. Gubbins, *Phys. Rev. E* **55**, R1290 (1997).
- [49] L. D. Gelb and K. E. Gubbins, *Phys. Rev. E* **56**, 3185 (1997).
- [50] L. D. Gelb, K. E. Gubbins, R. Radhakrishnan, and M. Sliwinskiabartkowiak, *Rep. Prog. Phys.* **62**, 1573 (1999).
- [51] J. W. Cahn, *J. Chem. Phys.* **66**, 3667 (1977).
- [52] P. G. de Gennes, *Rev. Mod. Phys.* **57**, 827 (1985).
- [53] M. Schick, in *Les Houches Session XLVIII, 1988*, edited by J. Charvolin (Amsterdam, Elsevier, 1990), p. 415.
- [54] L. E. Reichl, *A modern course in statistical physics* (John Wiley & Sons, New York, 1998).
- [55] J. S. Rowlinson, *Liquids and liquid mixtures* (Butterworth, London, 1969), 2nd ed.
- [56] T. Flebbe, B. Dünweg, and K. Binder, *J. Phys. II* **6**, 667 (1996).
- [57] W. H. Press, B. P. Flannery, S. A. Teukolsky, and W. T. Vetterling, *Numerical Recipes in Fortran* (Cambridge University Press, Cambridge, 1992), 2nd ed.
- [58] Z. Zhang, H. Zhang, and Y. Yang, *J. Chem. Phys.* **115**, 7783 (2001).
- [59] V. M. Kendon, M. E. Cates, I. Pagonabarraga, J. C. Desplat, and P. Bladon, *J. Fluid Mech.* **440**, 147 (2001).
- [60] when the gas is in the Knudsen regime, the slip length does not depend on the thickness of the boundary layer [30].